

Out-of-equilibrium Kondo Effect in a Quantum Dot: Interplay of Magnetic Field and Spin Accumulation

SHAON SAHOO^{1,2}, ADELIN CRÉPIEUX³ and MIREILLE LAVAGNA^{1,2,4}

¹ *Université Grenoble Alpes, INAC-PHELIQS - F-38000 Grenoble, France*

² *CEA, INAC-PHELIQS - F-38000 Grenoble, France*

³ *Aix Marseille Univ, Université de Toulon, CNRS, CPT - Marseille, France*

⁴ *Also at: Centre National de la Recherche Scientifique - CNRS - Grenoble, France.*

PACS 72.15.Qm – Scattering mechanisms and Kondo effect
PACS 73.25.Dc – Spin polarized transport in semiconductors
PACS 73.23.-b – Electronic transport in mesoscopic systems

Abstract – We present a theoretical study of low temperature nonequilibrium transport through an interacting quantum dot in the presence of Zeeman magnetic field and current injection into one of its leads. By using a self-consistent renormalized equation of motion approach, we show that the injection of a spin-polarized current leads to a modulation of the Zeeman splitting of the Kondo peak in the differential conductance. We find that an appropriate amount of spin accumulation in the lead can restore the Kondo peak by compensating the splitting due to magnetic field. By contrast when the injected current is spin-unpolarized, we establish that both Zeeman-split Kondo peaks are equally shifted and the splitting remains unchanged. Our results quantitatively explain the experimental findings reported in KOBAYASHI T. *et al.*, *Phys. Rev. Lett.* **104**, 036804 (2010). These features could be nicely exploited for the control and manipulation of spin in nanoelectronic and spintronic devices.

Introduction. – Progress in nano-fabrication opened the emergence of a new class of objects, semi-conductors quantum dots -QDs- in which a few electrons localized in a small spatial region are connected to leads through tunneling barriers. QDs are very attractive for electronic and spintronic applications due to the possibility they offer to control and manipulate the spin. They give the unique opportunity to observe a tunable Kondo effect at low temperature when the dot possesses an odd number of electrons and acquires a net spin $S=1/2$. The theoretical predictions of a Kondo effect in such nanostructures were made in the late 80s [1,2]. The Kondo effect is a many-body phenomenon which takes place when a localized impurity with an unpaired spin is embedded in a metallic host. It arises from resonant hopping processes of the conduction electrons of the host in and out of a localized impurity. This resonant process leads to the screening of the spin of the localized electrons with the formation of a Kondo singlet state. The binding energy of this singlet state defines the Kondo temperature T_K . It was predicted that the Kondo effect leads to an increase of the linear conductance of the QD when temperature is lowered below T_K . This feature

is the exact analog of the rise of resistivity brought by for the Kondo effect in bulk metals [3] when temperature is lowered below T_K . Experimentally the first observation of the Kondo effect in QDs was made in GaAs-based two-dimensional structures in the late 90s [4,5].

For any usefulness of nanoelectronic and spintronic devices, it is necessary to be able to control and manipulate the spin in these systems. In this perspective QDs are excellent candidates since their properties can be tuned in a controlled way by varying voltages. They can be placed in an out-of-equilibrium situation by applying a finite source-drain voltage V_D between the two leads (by convention source voltage V_S is considered as the ground potential). In the case of a single-level QD connected to normal metal leads, the differential conductance $g_D = dI_D/dV_D$ vs V_D exhibits a zero-bias anomaly [6]. In the presence of a Zeeman magnetic field Δ , the Kondo peak in the differential conductance is split with a value of the splitting of the order of $2\Delta/e$ as discussed in [5,7–9]. The transport properties of the QD can also be changed by modifying the environment of the dot. A case of special interest in connection to the study presented in this Letter corresponds

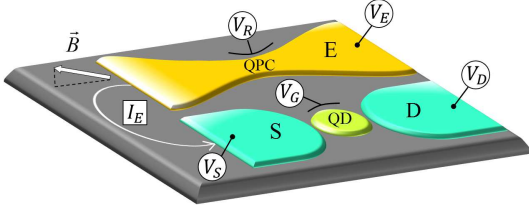


Fig. 1: Schematic representation of the experimental setup constituted by a QD connected to the two electrodes, source S and drain D, and a QPC responsible for the generation of the current I_E injected from the emitter E into S. An external magnetic field is applied to the system with the plane of the device tilted by a small angle to the axis of the magnetic field.

to QDs with ferromagnetic leads [10–13]. It was shown that spin-polarization in the leads results in an effective static magnetic field which splits the Kondo peak in g_D as observed experimentally. The Kondo peak may then be restored by compensating this effective magnetic field by a Zeeman magnetic field.

More recently there has been a considerable effort in developing new techniques to modify the environment to achieve efficient control of the spin in QDs. The injection of a current in one of the leads of a QD has emerged as a very powerful way to attain this goal with the possibility to produce a spin accumulation in the lead when the current is spin-polarized [14–18]. We especially refer to experimental work by Kobayashi *et al.* [18] whose experimental setup is schematized in fig. 1. The generation of the current is achieved with the aid of a quantum point contact -QPC- which is spin-polarized by applying a high parallel Zeeman magnetic field. The differential conductance of the QPC, $g_E = dI_E/dV_E$ vs gate voltage V_R is quantized [19] at multiples of e^2/h determined by the number of occupied subbands in the QPC. The current I_E induced by the application of a bias voltage V_E to the emitter E, is then magnetically focused [20] into S along the cyclotron trajectory by applying a low perpendicular magnetic field. In practice in order to apply a high parallel magnetic field for Zeeman splitting in both QPC and QD, and a low perpendicular magnetic field for magnetic focusing, the 2DEG plane is tilted by a small angle to the axis of the applied magnetic field.

The experimentalists have shown that the low temperature transport through a Kondo QD is considerably influenced by the injection of a current into one of its leads. The observations [18] show spectacular effects on the evolution of the differential conductance with V_D depending on the number of open transmission channels in the QPC which can be controlled by V_R . The profile of the Zeeman-split Kondo peaks versus V_E are found to have a very characteristic dependence on the nature of injected current. While a spin-polarized current affects the separation between the two peaks in the differential conductance, a spin-unpolarized current equally shifts both peaks. The

former case thus offers the possibility of recovering the Kondo peak by accumulating an appropriate amount of spin in one lead to compensate the Zeeman magnetic field effect.

On the theoretical side, the pioneering works go back to [17] and [21]. Qi *et al.* [17] examined the fate of the Kondo resonance peak in the density of states in the presence of a spin accumulation for systems with a local impurity embedded in a metal. By using an equation of motion (EOM) approach on the single impurity Anderson model -SIAM, they found that the Kondo resonance is split into two peaks pinned to the spin-dependent chemical potentials. They then showed that the Kondo resonance may be restored by applying an external magnetic field. Since they are bulk, these systems do not offer the possibility of applying a finite bias voltage across the impurity. Lim *et al.* [21] further considered the situation of quantum dots in the presence of static spin polarization of the contact and spin accumulation in the electrode as resulting from the injection of a spin-polarized current. By also using an equation of motion approach on the SIAM, they showed that spin polarization and spin accumulation have antagonist effects on the Kondo peak for both the spectral density and differential conductance. Whereas the spin-polarization of the contact is shown to introduce a splitting of the Kondo resonance, they demonstrated that the spin accumulation may compensate the latter splitting and restore the Kondo resonance. These two theoretical works have the merit of having highlighted the role that a spin accumulation can have on the Kondo effect. However we emphasize that their results have been obtained in the infinite U limit of the model. Moreover in [21], the truncated scheme considered within the EOM approach assumes $\langle f_{\sigma}^{\dagger} c_{k\alpha\sigma} \rangle = 0$ following Meir *et al.* [22, 23]. This assumption is known to be valid in the high temperature regime when $T \geq T_K$. By contrast it is important to have in mind that the whole set of results obtained by Kobayashi *et al.* has been obtained in the low temperature regime when $T \leq T_K$ in systems where the Coulomb interaction is estimated to 1.5 meV far from the infinite U limit. The results obtained therefore in the two theoretical works do not apply to the situation in which the experiments are performed.

The purpose of this Letter is precisely to fill this discrepancy and to study how the spin accumulation in one of the leads of a QD affects the transport properties of an interacting quantum dot in the low temperature and finite U regime. To do this we choose to carry out our theoretical study in conditions as close as possible to those in which the experiments were carried out. Our calculations based on the single impurity Anderson model at finite U are performed by using the self-consistent renormalized equation of motion approach following the scheme developed in [24, 25] in nonequilibrium situation. The decoupling scheme used to truncate the set of EOM considers the mixed decoupling parameter $\langle f_{\sigma}^{\dagger} c_{k\alpha\sigma} \rangle$ in addition to the usual decoupling parameters $\langle c_{k'\alpha\bar{\sigma}}^{\dagger} c_{k\alpha\bar{\sigma}} \rangle$ and $\langle n_{\bar{\sigma}} \rangle$.

This additional decoupling parameter plays a key role in the description of the strong coupling regime reached at low temperature. It can be viewed as a pseudo-order parameter which gets finite in the strong coupling regime, reminding of the slave-boson introduced in auxiliary-field approaches. Moreover the scheme includes two major improvements related to the renormalization of intermediate state inverse lifetimes and the renormalization of dot energy level, defining the self-consistent renormalized EOM approach. The renormalization of the intermediate state inverse lifetimes allows to cure the long-standing problem about the presence of a spurious peak in the density of states. This unphysical peak just compensates the actual Kondo resonance peak at the particle-hole symmetric point $\varepsilon_\sigma = -U/2$, therefore prohibiting one from studying the Kondo physics at this point. This serious drawback of the standard EOM approach is avoided in the self-consistent renormalized approach used in this work. Let us note that the particle-hole symmetric limit corresponds precisely to the situation in which the experimentalists have conducted their experiments where the system is placed at the middle of the Kondo conductance valley. Our calculations show that the splitting of the Kondo peak in the differential conductance is modulated by the shift of the chemical potentials introduced by spin injection. The results for the differential conductance vs V_D and V_E are found to be in quantitative agreement with the experimental results. We analyze them in detail by extracting the Kondo peak parameters and comparing them with the parameters extracted from experiments.

Model. — The QD is modeled by the single impurity Anderson model

$$H = \sum_{k,\alpha \in (S,D),\sigma} \varepsilon_{k\alpha\sigma} c_{k\alpha\sigma}^\dagger c_{k\alpha\sigma} + \sum_{\sigma} \varepsilon_{\sigma} f_{\sigma}^\dagger f_{\sigma} + U n_{\uparrow} n_{\downarrow} + \sum_{k,\alpha \in (S,D),\sigma} (t_{\alpha\sigma} c_{k\alpha\sigma}^\dagger f_{\sigma} + h.c.), \quad (1)$$

where $c_{k\alpha\sigma}^\dagger$ ($c_{k\alpha\sigma}$) creates (annihilates) an electron with momentum k , spin σ ($\sigma = \pm 1$) and energy $\varepsilon_{k\alpha\sigma}$ in the α lead. f_{σ}^\dagger (f_{σ}) creates (annihilates) an electron with spin σ and energy $\varepsilon_{\sigma} = \varepsilon_0 - \sigma\Delta/2$ in the dot where $\Delta = |g^* \mu_B B|$ is the absolute value of the Zeeman splitting with g^* the g -factor in GaAs [26] and μ_B the Bohr magneton. U is the on-site Coulomb interaction in the dot. $n_{\sigma} = f_{\sigma}^\dagger f_{\sigma}$ and $t_{\alpha\sigma}$ is the transfer matrix element between states, assumed to be k -independent.

In the steady state the current through the dot for spin σ is given by [27],

$$I_{D\sigma} = \frac{2e}{\hbar} \int_{-W}^{+W} d\omega \tilde{\Gamma}_{\sigma}(\omega) \times [n_F(\omega - \mu_{L\sigma}) - n_F(\omega - \mu_{R\sigma})] A_{\sigma}(\omega), \quad (2)$$

where $\tilde{\Gamma}_{\sigma}(\omega) = \frac{\Gamma_{L\sigma}(\omega)\Gamma_{R\sigma}(\omega)}{\Gamma_{L\sigma}(\omega) + \Gamma_{R\sigma}(\omega)}$ with the tunnel coupling constants given by $\Gamma_{\alpha\sigma}(\omega) = \pi |t_{\alpha\sigma}|^2 \rho_{\alpha\sigma}^0(\omega)$. $\rho_{\alpha\sigma}^0(\omega)$ is

the density of states in the α lead for spin σ and W is the half-bandwidth. $A_{\sigma}(\omega) = -\frac{1}{\pi} \text{Im} G_{\sigma}^r(\omega)$ and $G_{\sigma}^r(\omega)$ are respectively the spectral density and retarded Green function in the dot. $n_F(\omega - \mu_{\alpha\sigma}) = [\exp[(\omega - \mu_{\alpha\sigma})/k_B T] + 1]^{-1}$ is the Fermi-Dirac distribution function in the α lead with chemical potential $\mu_{\alpha\sigma}$. $\mu_{D\sigma} = \mu_0 - eV_D$ for both spin σ where μ_0 is the chemical potential at equilibrium. When the lead S is exposed to a current injection, the chemical potentials in S are selectively shifted depending on the value of g_E . When the QPC is tuned in the middle of the 0th plateau, $g_E = 0$, no current goes through the QPC and $\mu_{S\uparrow} = \mu_{S\downarrow} = \mu_0$. When the QPC is tuned in the middle of the 1st plateau, $g_E = e^2/h$, a spin-polarized current with only spin-up electrons is injected into S and $\mu_{S\uparrow} = \mu_0 - eV_E$ whereas $\mu_{S\downarrow} = \mu_0$. When the QPC is tuned in the middle of the 2nd plateau, $g_E = 2e^2/h$, the current is spin-unpolarized and $\mu_{S\uparrow} = \mu_{S\downarrow} = \mu_0 - eV_E$.

Equation of motion approach. — The spectral density, $A_{\sigma}(\omega)$, appearing in eq. (2) can be derived from $G_{\sigma}^r(\omega)$ which we evaluate using the EOM approach. Extensively used in the past to study bulk metals [28, 29] and quantum impurities in equilibrium [22], the EOM approach has been more recently extended to nonequilibrium [21, 23, 24, 30–35]. We use here the self-consistent renormalized EOM approach as developed in [24, 25]. In this approach the set of equations of motion of Green functions are truncated at the third level of the hierarchy by performing a decoupling in terms of all possible two-operator correlation functions with equal-spin, $\langle f_{\bar{\sigma}}^\dagger c_{k\alpha\bar{\sigma}} \rangle$, $\langle c_{k'\alpha\bar{\sigma}}^\dagger c_{k\alpha\bar{\sigma}} \rangle$ and $\langle n_{\bar{\sigma}} \rangle$ where $\bar{\sigma} = -\sigma$. We point out the importance of considering the mixed decoupling parameter $\langle f_{\bar{\sigma}}^\dagger c_{k\alpha\bar{\sigma}} \rangle$ -undeservedly neglected most often in the literature- to properly describe the strong coupling regime at low temperature. This leads to the following result [24]

$$G_{\sigma}^r(\omega) = \frac{1 - \langle n_{\bar{\sigma}} \rangle}{\omega - \varepsilon_{\sigma} - \Sigma_{\sigma}^0(\omega) - \Pi_{\sigma}^{(1)}(\omega)} + \frac{\langle n_{\bar{\sigma}} \rangle}{\omega - \varepsilon_{\sigma} - U - \Sigma_{\sigma}^0(\omega) - \Pi_{\sigma}^{(2)}(\omega)}, \quad (3)$$

where $\Sigma_{\sigma}^0(\omega) = -i\sigma(\omega)$ and $\Gamma_{\sigma}(\omega) = \sum_{\alpha=S,D} \Gamma_{\alpha\sigma}(\omega)$. In the wide band limit, $\Sigma_{\sigma}^0(\omega)$ is independent of ω taking the value $-i\Gamma_{\sigma}$. $\Pi_{\sigma}^{(1)}(\omega)$ and $\Pi_{\sigma}^{(2)}(\omega)$ are defined as

$$\Pi_{\sigma}^{(1)}(\omega) = -U \frac{\Sigma_{\sigma}^{(1)}(\omega) - (\omega - \varepsilon_{\sigma}) \Sigma_{\sigma}^{(4)}(\omega)}{\omega - \varepsilon_{\sigma} - U - \Sigma_{\sigma}^{(3)}(\omega) + U \Sigma_{\sigma}^{(4)}(\omega)} \quad (4)$$

$$\Pi_{\sigma}^{(2)}(\omega) = U \frac{\Sigma_{\sigma}^{(2)}(\omega) + (\omega - \varepsilon_{\sigma} - U) \Sigma_{\sigma}^{(4)}(\omega)}{\omega - \varepsilon_{\sigma} - \Sigma_{\sigma}^{(3)}(\omega) + U \Sigma_{\sigma}^{(4)}(\omega)}, \quad (5)$$

where

$$\Sigma_{\sigma}^{(i)}(\omega) = \sum_{k,\alpha} |t_{\alpha\bar{\sigma}}|^2 \left[\frac{A_{k\alpha\bar{\sigma}}^{(i)}}{\omega + \tilde{\varepsilon}_{\bar{\sigma}} - \tilde{\varepsilon}_{\sigma} - \varepsilon_{k\alpha\bar{\sigma}} + i\tilde{\gamma}_{\sigma}} + \frac{A_{k\alpha\sigma}'^{(i)}}{\omega + \tilde{\varepsilon}_{k\alpha\bar{\sigma}} - \tilde{\varepsilon}_{\sigma} - \tilde{\varepsilon}_{\bar{\sigma}} - U + i\tilde{\gamma}_D} \right], \quad (6)$$

with $A_{k\alpha\sigma}^{(1)} = \sum_{k'} \langle c_{k'\alpha\bar{\sigma}}^\dagger c_{k\alpha\bar{\sigma}} \rangle$, $A_{k\alpha\sigma}^{(2)} = 1 - \sum_{k'} \langle c_{k'\alpha\bar{\sigma}}^\dagger c_{k\alpha\bar{\sigma}} \rangle$, $A_{k\alpha\sigma}^{(3)} = 1$, and $A_{k\alpha\sigma}^{(4)} = \langle f_\sigma^\dagger c_{k\alpha\bar{\sigma}} \rangle / t_{\alpha\bar{\sigma}}$. $A_{k\alpha\sigma}^{(i)} = (A_{k\alpha\sigma}^{(i)})^*$ for $i = 1, 2, 3$ and $A_{k\alpha\sigma}^{(4)} = -(A_{k\alpha\sigma}^{(4)})^*$.

Expression (3) for $G_\sigma^r(\omega)$ is exact both in the non-interacting limit ($U = 0$) and in the isolated-site limit ($t_{\alpha\sigma} = 0$). The expression exhibits two poles at ε_σ and $(\varepsilon_\sigma + U)$ corresponding to the isolated-site limit, weighted by the factors $(1 - \langle n_{\bar{\sigma}} \rangle)$ and $\langle n_{\bar{\sigma}} \rangle$ respectively. $\Sigma_\sigma^0(\omega)$ is the ordinary self-energy due to electron tunneling between the dot and the leads, whereas $\Pi_\sigma^{(1)}(\omega)$ and $\Pi_\sigma^{(2)}(\omega)$ are the self-energy contributions due to interactions. Expression (3) constitutes an extension of Lacroix' [29] and Meir et al.'s [22] results. At equilibrium and in the infinite U limit, the expression gives back the results of [29]. When $\langle f_\sigma^\dagger c_{k\alpha\bar{\sigma}} \rangle = 0$ (and hence $\Sigma_\sigma^{(4)}(\omega) = 0$), the results of [22] are recovered, corresponding to the high temperature limit. The consideration of this extra-parameter $\langle f_\sigma^\dagger c_{k\alpha\bar{\sigma}} \rangle$ is crucial to describe the low-temperature limit. It ensures the unitary condition for $G_\sigma^r(\omega)$ at the Fermi level to be fulfilled at zero temperature [24, 25, 29]. The decoupling parameters $\langle f_\sigma^\dagger c_{k\alpha\bar{\sigma}} \rangle$, $\langle c_{k'\alpha\bar{\sigma}}^\dagger c_{k\alpha\bar{\sigma}} \rangle$, and $\langle n_{\bar{\sigma}} \rangle$ are then determined by the self-consistent equations established both at and out-of-equilibrium [24] provided that the system is in a steady state. As a result the self-energies $\Sigma_\sigma^{(i)}(\omega)$ are expressed in terms of $G_\sigma^r(\omega)$. The Green function $G_\sigma^r(\omega)$ can then be self-consistently calculated from eq. (3).

We consider two important improvements related to the renormalization of both intermediate state inverse lifetimes and dot energy level. These two improvements define the self-consistent renormalized EOM approach where propagators and vertices of the corresponding skeleton Feynman diagrams are dressed by self-energy and vertex corrections respectively. In the standard EOM approach, $\tilde{\varepsilon}_\sigma$ is the bare energy level ε_σ in the dot, and $\tilde{\gamma}_\sigma$ and $\tilde{\gamma}_D$ are both an infinitesimal positive ($\gamma_\sigma = \gamma_D = +i\delta$). They are renormalized in the self-consistent renormalized EOM approach. On the one hand, $\tilde{\varepsilon}_\sigma$ is renormalized by self-energy corrections according to: $\tilde{\varepsilon}_\sigma = \varepsilon_\sigma + \Re \Sigma_\sigma^{(1)}(\omega = \tilde{\varepsilon}_\sigma)$. At the particle-hole symmetric point the renormalization effect on $\tilde{\varepsilon}_\sigma$ is zero and $\tilde{\varepsilon}_\sigma = \varepsilon_\sigma$. On the other hand $\tilde{\gamma}_\sigma$ and $\tilde{\gamma}_D$ are replaced by the inverse lifetimes of intermediate states. They are determined by using the generalized Fermi golden rules up to the forth order in $t_{\alpha\sigma}$ following [24, 25], extending to finite U the argument used in [23] for the infinite- U limit. The renormalization of $\tilde{\gamma}_D$ proves to be extremely important to cure the long-standing problem about the presence of a spurious peak in the density of states. This unphysical peak, which compensates the actual Kondo resonance peak, is the reason behind the failure of the standard EOM approaches. This drawback is avoided in the self-consistent renormalized EOM approach used in this work. By using Eqs. (2-6), we have all the ingredients to derive the total current I_D and the differential conductance $g_D = dI_D/dV_D$.

Choice of parameters and Kondo temperature. –

Except for U , the values of all the parameters inserted in our model are adopted from the estimations made in [18]. Hence the electronic temperature is taken as $T = 100$ mK, $\Delta = 130$ μ eV and $\Gamma_{\alpha\sigma} = 0.25$ meV. As far as U is concerned, we choose to take a slightly larger value $U = 3$ meV instead of $U = 1.5$ meV considered in [18] to ensure that the system is in the Kondo regime on the following criterion: $2\Gamma_{\alpha\sigma} \ll U/2$. Besides we consider the system at the particle-hole symmetric point with $\varepsilon_0 = -U/2$ in agreement with the experimental situation.

The Kondo temperature, T_K , of the QD is estimated from the linear conductance vs temperature plotted at equilibrium (for $B = V_E = 0$). T_K is the temperature at which the linear conductance falls down to half of its maximum value. We get: $T_K = 0.5$ K. Upper bounds to T_K can be found in various nonequilibrium situations. For example, an upper bound to T_K is estimated from the value of the FWHM of the Kondo peak in g_D vs V_D plot. We perform calculations at $T = 100$ mK (for $B = V_E = 0$), and get $T_K < 0.7$ K. Finally the value of T_K estimated from Haldane's formula [36] is 0.9 K. These values are consistent with the upper bound 0.7 K estimated in experiment [18] even though we have taken a slightly different value of U . Let us also mention that all our numerical calculations are performed at 100 mK, well below the estimated T_K .

Results and discussion. – Our numerical results for the differential conductance g_D are represented in both gray-scale representation in the plane (V_D, V_E) in figs. 2(c)-2(d), and in g_D vs V_D plots in figs. 2(e)-2(f) at $g_E = e^2/h$ and $g_E = 2e^2/h$ respectively. We do not show the result for $g_E = 0$ since g_D vs V_D plot is simply the one obtained for $g_E \neq 0$ at $V_E = 0$. As can be seen from figs. 2(e)-2(f), generally g_D vs. V_D has two peaks. The variations of the positions of the peaks with V_E depend on the spin-polarization state of the injected current. At $V_E = 0$ the Kondo peaks occur at $V_D = \pm\Delta/e$ as expected. When the injected current is spin-polarized (by tuning the QPC at $g_E = e^2/h$), the position of the upper- V_D peak does not vary with V_E whereas that of the lower- V_D peak is linearly shifted by V_E . The separation between the two peaks decreases with increasing positive V_E until vanishing at a critical value of V_E . When the injected current is spin-unpolarized (by tuning the QPC at $g_E = 2e^2/h$), the positions of both peaks are equally shifted by V_E .

With the aim of understanding the physical mechanisms behind these results, we illustrate in figs. 2(a)-2(b) the schematic representation of the energy level diagram in the QD at $g_E = e^2/h$ and $g_E = 2e^2/h$ respectively, for finite V_D , V_E and Δ . From eq. (3) it is easy to see that the spectral density $A_\sigma(\omega)$ exhibits two Kondo peaks at about $(\mu_{\alpha\bar{\sigma}} + \varepsilon_\sigma - \varepsilon_{\bar{\sigma}}) = \mu_{\alpha\bar{\sigma}} - \sigma\Delta$ for each α [37]. Following eq. (2), g_D vs V_D exhibits a peak whenever one of the chemical potentials for a given spin gets aligned with a Kondo DOS peak for the same spin. This occurs when $\mu_{\beta\sigma} = (\mu_{\alpha\bar{\sigma}} + \varepsilon_\sigma - \varepsilon_{\bar{\sigma}})$, leading to the ana-

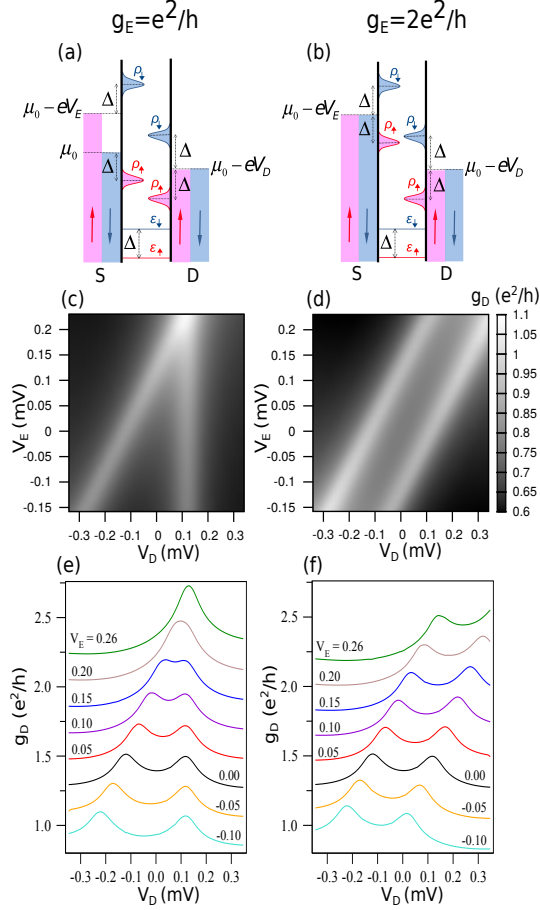


Fig. 2: (a)-(b) Schematic representation of the energy level diagram in the QD at $g_E = e^2/h$ and $g_E = 2e^2/h$ for finite V_D , V_E and Δ . ρ_\uparrow (ρ_\downarrow) represent the Kondo peaks in $A_\uparrow(\omega)$ ($A_\downarrow(\omega)$). (c)-(d) Results for the differential conductance g_D in gray-scale representation in the plane (V_D, V_E) at $g_E = e^2/h$ and $g_E = 2e^2/h$. (e)-(f) Results for the differential conductance g_D vs V_D at $g_E = e^2/h$ and $g_E = 2e^2/h$ for V_E ranging from -0.10 mV (bottom) to 0.26 mV (top). The curves are vertically offset by $0.2e^2/h$ for clarity. The results are obtained for the symmetric Anderson model at $T = 100$ mK with $U = 3$ meV, $\Gamma_{\alpha\sigma} = 0.25$ meV and $\Delta = 0.13$ meV.

lytic prediction for the positions of the Kondo peaks. At $g_E = 0$ the Zeeman-split Kondo peak is found to occur at $V_D = \pm(\epsilon_\sigma - \epsilon_{\bar{\sigma}})/e = \pm\Delta/e$. The splitting is equal to $2\Delta/e$. At $g_E = e^2/h$, the two Kondo peaks are found to be located at $V_D = -\Delta/e + V_E$ and $V_D = \Delta/e$. The separation between these two peaks is $(2\Delta/e - V_E)$, which decreases with increasing V_E . When $V_E = 2\Delta/e$, the Zeeman splitting of the Kondo peak is exactly compensated by spin accumulation in the lead produced by the injection of a spin-polarized current. At this compensation point, the two peaks merge into a single peak and the Kondo peak is restored. This manifestation can be viewed as the fingerprint of the formation of the Kondo spin-singlet state at low temperature. At $g_E = 2e^2/h$, the analytic predictions for the positions of the two Kondo peaks are

$V_D = -\Delta/e + V_E$ and $V_D = \Delta/e + V_E$. The separation between peaks is $2\Delta/e$, independent of V_E .

In order to extract the peak parameters from our numerical results, we fit the curves in figs. 2(e)-2(f) by a double-Lorentzian function with a quadratic background according to: $f(x) = a + bx + cx^2 + z_1 \left[\frac{1}{\pi} \frac{w_1/2}{(x-x_1)^2 + (w_1/2)^2} \right] + z_2 \left[\frac{1}{\pi} \frac{w_2/2}{(x-x_2)^2 + (w_2/2)^2} \right]$. The quadratic background is necessary to account for the contributions of the two broad charge peaks in the DOS. We take two different weight factors z_1 and z_2 to account for the asymmetry in the spectral density arising mainly from charge accumulation in S when $V_E \neq 0$. The extracted values for peak positions x_i ($i=1,2$), FWHMs w_i , heights $2z_i/(\pi w_i)$ and weight factors z_i are reported in fig. 3. It is worth noticing that the parameter extraction is possible only up to $V_E = 0.15$ mV. Beyond this value the two peaks are too close and can no longer be resolved. As expected, w_i , heights and weight factors of the two peaks coincide at $V_E = 0$ in both cases. In fig. 3, P_1 and P_2 correspond respectively to the lower- V_D and upper- V_D peaks at $g_E = e^2/h$ whereas P_3 and P_4 are the equivalent peaks at $g_E = 2e^2/h$. As can be seen in fig. 3(a), our numerical results for the peak positions (in solid lines) are in excellent agreement with our analytical predictions of $V_D = V_E \pm \Delta/e$ and $V_D = \Delta/e$ (in broken lines). The extracted FWHMs vs V_E for the different peaks are reported in fig. 3(b). The values of the FWHM give us some useful information about the degree of decoherence in the Kondo resonance. The higher V_D , Δ or $(\mu_{\alpha\sigma} - \mu_0)$, the higher the FWHM. As can be seen from fig. 3(b), w_i for both P_1 and P_2 saturate at large positive values of V_E when the system gets closer to the compensation point where the Kondo peak is restored. From the same figure, one can see that w_i for P_3 and P_4 do not show any evidence of saturation at large values of V_E as expected. Finally the extracted peak heights and weight factors vs V_E are reported in figs. 3(c)-3(d). While the peak height results from the two antagonistic effects brought by z_i and $1/w_i$ contributions respectively, the results show that the dominant contribution is provided by z_i .

The orders of magnitude of the various peak parameters and their overall evolution as a function of V_E are in good agreement with the experimental data [18] although the value that we adopted for U is slightly different from the experimental estimation. However we would like to point out that unlike what we find in our calculations, the experimental results show a deflection of the P_2 line from $V_D = \Delta/e$ in the vicinity of the Kondo compensation point along with large and sudden fluctuations of the FWHMs for both P_1 and P_2 in this range. One of the reasons for this behavior as suggested in Ref. [18] is that the system is in a highly nonequilibrium situation when $g_E = e^2/h$ and hence the fermion states below $\mu_{S\uparrow}$ along the cyclotron trajectory from E to S, are not fully occupied at zero temperature [38, 39]. This would result in a double-step instead of the single-step Fermi-Dirac distri-

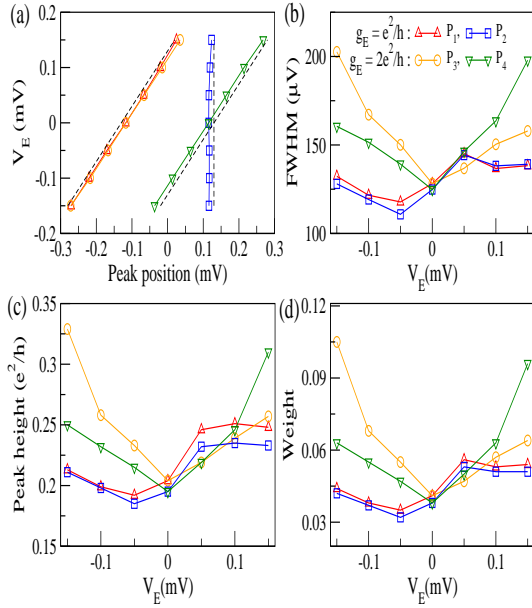


Fig. 3: Kondo peak parameters extracted from results for g_D vs V_D . (a) Peak positions. The extracted peak positions are represented in solid lines whereas our analytical predictions $V_D = V_E \pm \Delta/e$ and $V_D = \Delta/e$ are represented in broken lines. (b) FWHMs. (c) Peak heights. (d) Weight factors.

bution function considered in our calculations. It would be interesting in the future to investigate consequences of this situation.

Conclusion. — In summary, we have studied the combined effects of Zeeman magnetic field and current injection into one lead on the nonlinear conductance of a QD in the low temperature regime. When the injected current is spin-polarized, the Zeeman splitting of the Kondo peak in the differential conductance is found to be compensated by an appropriate amount of spin accumulation in the lead and the Kondo peak is restored in good agreement with experimental data [18]. Our results in this Letter show that the injection of a current in one lead of a QD offers a new and promising route to controlling and manipulating spin in nanoelectronic devices. Present work opens the possibility of studying other important situations such as separate spin accumulations in both leads with or without the presence of magnetic field. In the absence of magnetic field, we predict that the Kondo peak is restored when the two leads have an equal amount of spin accumulation with opposite spin orientation.

We would like to thank H. Baranger for valuable discussions. For financial support, the authors acknowledge the Indo-French Centre for the Promotion of Advanced Research (IFCPAR) under Research Project No.4704-02 and the Nanosciences Foundation of Grenoble under Contract CORTANO.

REFERENCES

- [1] NG T.K. and LEE P.A., *Phys. Rev. Lett.*, **61** (1988) 1768.
- [2] GLAZMAN L. and RAIKH M., *JETP Lett.*, **11** (1988) 2389.
- [3] HEWSON A.P., *The Kondo Problem to Heavy Fermions* (Cambridge University Press) 1993 and references therein.
- [4] GOLDBABER-GORDON D., SHTRIKMAN H., MAHALUD., ABUSCH-MAGDER D., MEIRAV U. and KASTNER M., *Nature*, **61** (1998) 156.
- [5] CRONENWETT S.M., OOSTERKAMP T.H. and KOUWENHOVEN L.P., *Science*, **281** (1998) 165115.
- [6] VAN DER WIEL W., DE FRANCESCHI S., FUJISAWA T., ELZERMANN J., TARUCHA S. and KOUWENHOVEN L.P., *Science*, **289** (2000) 2105.
- [7] COSTI T.A., *Phys. Rev. Lett.*, **85** (2000) 1504.
- [8] ROSCH A., PAASKE J., KROHA J. and WÖLFLE P., *Phys. Rev. Lett.*, **90** (2003) 076804.
- [9] HEWSON A.C., BAUER J. and OGURI A., *J. Phys.: Condens. Matter*, **17** (2005) 5413.
- [10] ZHANG P., XUE Q.-K., WANG Y.P. and XIE X.C., *Phys. Rev. Lett.*, **89** (2002) 286803.
- [11] MARTINEK J., UTSUMI Y., IMAMURA H., BARNAŠ J., MAEKAWA S., KÖNIG and SCHÖJ.G., *Phys. Rev. Lett.*, **91** (2003) 127203.
- [12] CHOI M.-S., SÁNCHEZ D. and LÓPEZ R., *Phys. Rev. Lett.*, **92** (2004) 056601.
- [13] KRAWIEC M., *J. Phys.: Condens. Matter*, **19** (2007) 346234.
- [14] POTOK R.M., FOLK J.A., MARCUS C.M. and UMANSKY V., *Phys. Rev. Lett.*, **89** (2002) 266602.
- [15] TANIYAMA T., FUJIWARA N., KITAMOTO Y. and YAMAZAKI Y., *Phys. Rev. Lett.*, **90** (2003) 016601.
- [16] KATSURA H., *J. Phys. Soc. Jpn.*, **76** (2007) 054710.
- [17] QI Y., ZHU J.-X., ZHANG S. and TING C.S., *Phys. Rev. B*, **78** (2008) 045305.
- [18] KOBAYASHI T., TSURUTA S., SASAKI S., FUJISAWA T., TOKURA Y. and AKAZAKI T., *Phys. Rev. Lett.*, **104** (2010) 036804.
- [19] VAN WEES B.J., KOUWENHOVEN L.P., VAN HOUTEN H., BEENAKKER C.W.J., MOOIJ J.E., FOXON C.T. and HARRIS J.J., *Phys. Rev. B*, **38** (1988) 3625.
- [20] VAN HOUTEN H., BEENAKKER C.W.J., WILLIAMSON J.G., BROEKAART M.E.I., VAN LOOSDRECHT P.H.M., VAN WEES B.J., MOOIJ J.E., FOXON C.T. and HARRIS J.J., *Phys. Rev. B*, **39** (1989) 8556.
- [21] LIM J.S., LÓPEZ R., LIMOT L. and SIMON P., *Phys. Rev. B*, **88** (2013) 165403.
- [22] MEIR Y., WINGREEN N.S. and LEE P.A., *Phys. Rev. Lett.*, **66** (1991) 3048.
- [23] MEIR Y., WINGREEN N.S. and LEE P.A., *Phys. Rev. Lett.*, **70** (1993) 2601.
- [24] LAVAGNA M., *Journal of Physics: Conference Series*, **592** (2015) 012141.
- [25] LAVAGNA M., *Nonequilibrium quantum transport through an interacting quantum dot*, in preparation.
- [26] Note the minus sign in front of $\sigma\Delta/2$ in the expression of ε_σ due to the fact that $g^* = -0.44$ in GaAs.
- [27] MEIR Y. and WINGREEN N.S., *Phys. Rev. Lett.*, **68** (1992) 2512.
- [28] APPELBAUM J.A. and PENN D.R., *Phys. Rev. B*, **188** (1969) 874.
- [29] LACROIX C., *J. Phys. F: Met. Phys.*, **11** (1981) 2389.

- [30] ENTIN-WOHLMAN O., AHARONY A. AND MEIR Y., *Phys. Rev. B*, **71** (2005) 035333 .
- [31] MONREAL R.C. and FLORES F. , *Phys. Rev. B*, **72** (2005) 195105.
- [32] KASHCHEYEV V., AHARONY A. and ENTIN-WOHLMAN O., *Phys. Rev. B*, **73** (2006) 125338.
- [33] ŚWIRKOWICZ R., WILCZYŃSKI M. and BARNAS J., *J. Phys.: Condens. Matter*, **18** (1988) 2006.
- [34] QI Y., ZHU J.X. and TING C.S., *Phys. Rev. B*, **79** (2009) 205110 .
- [35] VAN ROERMUND R., SHIAU S.Y. and LAVAGNA M. , *Phys. Rev. B*, **81** (2010) 165115.
- [36] HALDANE F.D.M., *Phys. Rev. Lett.*, **40** (1978) 416.
- [37] The fact that the Kondo peak in the density of states $A_\sigma(\omega)$ occurs at $(\mu_{\alpha\bar{\sigma}} - \sigma\Delta)$ reflects the formation of the Kondo spin-singlet state at low temperature.
- [38] DE FRANCESCHI S., HANSON R., VAN DER WIEL W.G., ELZERMAN J.M., WIJPKEMA J.J., FUJISAWA T., TARUCHA S. and KOUWENHOVEN L.P., *Phys. Rev. Lett.*, **89** (2002) 156801.
- [39] POTHIER H., GUÉRON S., BIRGE N.O., ESTÈVE D. and DEVORET M.H., *Phys. Rev. Lett.*, **79** (1997) 3490 .